Spin nematic interaction in multiferroic compound $Ba_2CoGe_2O_7$

M. Soda
Neutron Science Laboratory, Institute for Solid State Physics, University of Tokyo, Tokai, Ibaraki 319-1106, Japan

M. Matsumoto
Department of Physics, Shizuoka University, Shizuoka 422-8529, Japan

M. Månsson
Laboratory for Quantum Magnetism (LQM), École Polytechnique Fédérale de Lausanne (EPFL), Station 3, CH-1015 Lausanne, Switzerland and Laboratory for Neutron Scattering, Paul Scherrer Institut, CH-5232 Villigen PSI, Switzerland

S. Ohira-Kawamura and K. Nakajima
Materials and Life Science Division, J-PARC Center, Tokai, Ibaraki 319-1195, Japan

R. Shiina
Department of Materials Science and Technology, Niigata University, Niigata 950-2181, Japan

T. Masuda*
Neutron Science Laboratory, Institute for Solid State Physics, University of Tokyo, Tokai, Ibaraki 319-1106, Japan

(Dated: February 27, 2014)

We demonstrate the existence of the spin nematic interactions in an easy-plane type antiferromagnet $Ba_2CoGe_2O_7$ by exploring the magnetic anisotropy and spin dynamics. Combination of neutron scattering and magnetic susceptibility measurements reveals that the origin of the in-plane anisotropy is an antiferro-type interaction of the spin nematic operator. The relation between the nematic operator and the electric polarization in the ligand symmetry of this compound is presented. The introduction of the spin nematic interaction is useful to understand the physics of spin and electric dipole in multiferroic compounds.

arXiv:1402.6436v1 [cond-mat.str-el] 26 Feb 2014

Symmetry breaking of time reversal and space inversion allows spontaneous order both in magnetism and dielectricity[1]. The enhanced simultaneous order, multiferroics[2, 3], has been extensively studied since the discovery of its experimental realization in the perovskite manganite $TbMnO_3$[4]. The microscopic consideration of electronic states taking into account a spin-orbit (SO) interaction and symmetry of crystals reveals the relationship between the structures of spin $\boldsymbol{S}$ and polarization $\boldsymbol{P}$[5–9]. So far, in many multiferroic materials, the stability of complex spin orders has been focused in relation with induced electric polarizations. On the other hand, existence of an interaction among electric polarizations and its interplay with the spin interaction still remains unclear. In this context, a new material $Ba_2CoGe_2O_7$ provides a simple and quite interesting playground in which the polarizations are described by a rank two symmetric tensor of local spin operators, reflecting a symmetry of the tetrahedral unit involving the magnetic Co ions. One may call the spin representation of the polarization nematic or quadrupole, and can analyze their interaction on an equal footing with the spin exchange interaction. The main purpose of this paper is to give convincing evidence of realizing the nematic interaction and to clarify its crucial role in the magnetic anisotropy and the low energy physics in $Ba_2CoGe_2O_7$.

Two-dimensional square lattice antiferromagnet $Ba_2CoGe_2O_7$ includes metal-ligand motif with high symmetry but without inversion center. The crystal structure is tetragonal $P\bar{4}2_1m$ as schematically shown in Fig. 1(a). Co^{2+} ions carry spin $S = 3/2$ and the CoO_4 tetrahedron is distorted along the c direction. The compound exhibits an antiferromagnetic transition at T_N=6.7 K [10] and a staggered antiferromagnetic structure in the (001) plane with slight canting[11]. Below T_N, an electric polarization induced by a magnetic field is observed[12–14]. The origin of the polarization was explained by a spin-dependent d-p hybridization mechanism[12].

The electrons in the Co ion at the center of an isolated O_4 tetrahedron suffer from a crystal field potential of the point group D_{2d}. In this case, as we shall show later, conventional spin interaction does not break the spin rotation symmetry in the plane (001). In the present study, however, the combination of inelastic neutron scattering with high energy resolution and magnetic susceptibility measurements in $Ba_2CoGe_2O_7$ reveals existence of the distinct anisotropy in the plane. We argue through the following study that an unconventional nematic interaction is the origin of the anisotropy.

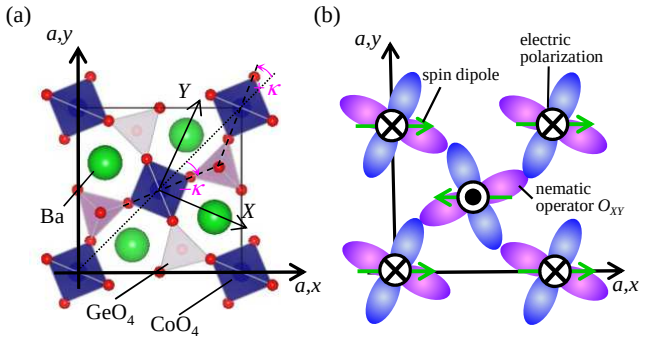

FIG. 1. (a) Crystal structure of $Ba_2CoGe_2O_7$. CoO_4 tetrahedra separated by GeO_4 tetrahedra form a square lattice in the (001) plane. The x and y axes in the global coordinate of spin are defined along [100] and [010] directions. The X and Y axes are locally defined on each CoO_4 tetrahedron. (b) Structures of spin dipoles, spin nematic operator O_{XY}, and electric polarizations at zero magnetic field in $Ba_2CoGe_2O_7$.

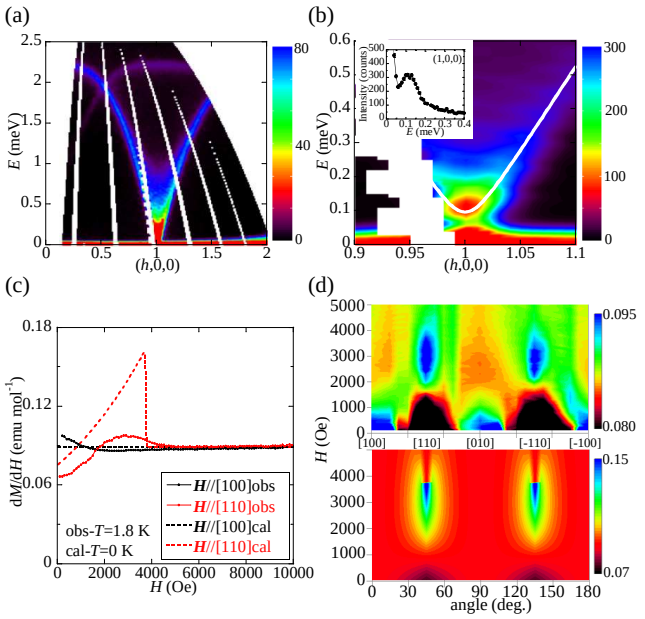

FIG. 2. (a) Inelastic neutron scattering spectrum obtained by using AMATERAS spectrometer in J-PARC. Well-defined spin-wave excitations are observed. (b) Inelastic neutron scattering spectrum in low energy range. The calculated dispersion is shown by the white solid curve. The inset shows the constant-Q scan at $\mathbf{Q}=(1,0,0)$. (c) Bulk susceptibility $\mathrm{d}M/\mathrm{d}H$ measured at $T = 1.8$ K. Red and black symbols indicate the $\mathrm{d}M/\mathrm{d}H$ for $H \parallel [110]$ and $H \parallel [100]$, respectively. Field cool processes are shown. Red and black dashed curves indicate the $\mathrm{d}M/\mathrm{d}H$ at $T = 0$ K calculated by mean-field theory. (d) The measured angular dependence of $\mathrm{d}M/\mathrm{d}H$ in upper panel and the calculated ones in lower panel.

Stoichiometric quantities of $BaCO_3$, CoO, and GeO_2 powders were mixed, and sintered at 900 °C for 24 h. The obtained powder is pressed into rods and they were sintered at 1,000 °C for 24 h. Using these rods as starting materials, single crystals were grown in air at a rate of 1 mm/h by floating zone method. Typical dimension of the crystals is about 8 mm in diameter and 40 mm in length. We confirmed absence of impurity phase by using powder X-ray diffractometer. Bulk magnetization was measured using a conventional SQUID magnetometer. Neutron measurements were carried out using the cold-neutron triple axis spectrometer TASP installed at SINQ/PSI, Switzerland. Throughout this paper, we use the tetragonal unit cell with a=b=8.410 Å and c=5.537 Å. The scattering plane was the a - c plane. The final neutron energy was set at 5 meV. The magnetic fields were applied along a direction vertical to the scattering plane (magnetic field $H//[010]$) using a superconducting magnet. Neutron measurements were also carried out using cold-neutron disk-chopper spectrometer AMATERAS of direct geometry type installed at J-PARC, Japan. The chopper condition was set so that the incident neutron energies E_i was 3.14meV and the resolutions of the energy transfer at the elastic position was 0.075meV.

In Fig. 2(a) the neutron spectrum is shown and a couple of spin-wave modes with the band energy of 2.2 meV are observed. Focused on the low energy range a clear anisotropy gap of approximately 0.10 meV at the antiferromagnetic zone center $\boldsymbol{Q} = (1,0,0)$ is observed in Fig. 2(b). The magnetic susceptibilities $\mathrm{d}M/\mathrm{d}H$ in field applying along [100] and [110] directions are shown in Fig. 2(c). In the latter a peak due to a spin flop (SF) transition is observed at $H \sim 3$ kOe that is consistent with the energy scale of the anisotropy gap, while in the former the SF transition is absent. The angular dependence of $\mathrm{d}M/\mathrm{d}H$ is summarized in the upper panel of Fig. 2(d), where four-fold rotational symmetry with the enhanced SF field at [110] and [−110] is observed. The presence of the four-fold in-plane anisotropy is consistent with the prediction of the anisotropy by investigating the crystallographic symmetry[15, 16].

In general the origin of the magnetic anisotropy gap in the excitation spectrum is a single-ion anisotropy or a two-ions anisotropy. The single-ion anisotropy in the spin state in this material is represented by the form $D(S^z)^2$ where the z-axis is the crystallographic c-axis. We note that there is no E term in the tetragonal system. The sign of D is believed to be positive since the direction of spins in the ordered state is perpendicular to the c-axis. Spin operators with 4th or higher order is inactive for S=3/2 in the local symmtery and, thus, the single ion anisotropy cannot lead to any in-plane anisotropy. Consider next the non-local symmetry of Co ions located on the $2a$ Wyckoff positions in the space group $P\bar{4}2_1m$ and the allowed two-ion anisotropy represented by a spin-dipole interaction is an XXZ-type one $J^x(S_1^xS_2^x + S_1^yS_2^y) + J^zS_1^zS_2^z$. The anisotropy is, again, does not break the rotational symmetry in the c-

plane nor induce the anisotropy gap. Among the two-ion anisotropies that break the rotational symmetry, the one having the lowest order is represented by the interaction between spin-nematic (quadrupole) operators , of which the exact formula will be obtained later. This means that in $Ba_2CoGe_2O_7$ the spin-nematic interaction is the leading term for rotational symmetry broken and, hence, the origin of the observed anisotropy gap is the spin-nematic interaction.

The representation of spin-nematic interaction is obtained by considering the electric polarization interaction. In $Ba_2CoGe_2O_7$ the spin nematic operator becomes equivalent to the polarization owing to the lack of the inversion symmetry in the D_{2d} point group symmetry of the CoO_4 tetrahedron[17, 18]. Thus, $P^X = -K_{ab}O_{YZ}$, $P^Y = -K_{ab}O_{ZX}$, and $P^Z = -K_cO_{XY}$, where K_{ab} and K_c are constants and X, Y, and Z are the local coordinates on CoO_4 tetrahedron as shown in Fig. 1(a)[19]. Here the spin nematic operator is defined as $O_{\alpha\beta} = S^\alpha S^\beta + S^\alpha S^\beta$, where $\{\alpha, \beta\} = \{X, Y, Z\}$. Let us consider the electrostatic polarization interaction on the basis of these operators. Among these, O_{YZ} and O_{ZX} become zero under the spin structure aligned in the ab-plane, while O_{XY} is finite. Then, only the Z component, $P^Z \propto O_{XY}$, is active and an intersite interaction of P^Z is converted to a nematic interaction of O_{XY} with an effective coupling strength $J_p^{\rm eff}$[17]. The explicit form is

$$\mathcal{H}_p = -J_p \sum_{i,j} P^Z(i)P^Z(j) = -J_p^{\rm eff} \sum_{i,j} O_{XY}(i)O_{XY}(j). \tag{1}$$

Thus, intersite polarization interaction gives rise to the interaction between the spin nematic operators. After the transformation to the global xy coordinates, we obtain

$$O_{XY} = \left(\cos(2\kappa)O_{xy} - \sin(2\kappa)O_2^2\right), \tag{2}$$

where $O_{xy} = S^xS^y + S^yS^x$ and $O_2^2 = (S^x)^2 - (S^y)^2$[17, 20]. The definition of the angle κ is described in Fig. 1 (a). Calculation of the classical energy including antiferromagnetic spin interaction and the nematic interaction between O_{XY} operators result in a ground state with staggered spin structure with four-fold rotational symmetry. Thus the existence of the nematic interaction explains the biaxial magnetic anisotropy in our experiment.

The sign of J_p and the magnetic-easy axes are determined from the angular dependence of the SF (spin flop) field $H_{\rm SF}$. In zero field there are four magnetic domain states; two of them share the magnetic easy axis and so do the rest two. The direction of the axis is orthogonal to each other. If the field is applied along one of the easy axes the spins in a domain of which the easy axis is parallel to the field flip instantly and those in another domain stay as they are. Hence the value of $H_{\rm SF}$ is zero or strongly suppressed. As the field direction tilts from the easy axes the Zeeman energy required for the SF increases and consequently $H_{\rm SF}$ is enhanced. Experimentally the minimum of $H_{\rm SF}$ is observed at $H \parallel [010]$ and [100] and this means that the easy axes are [010] and [100]. This magnetic anisotropy leads the negative sign of J_p in Eq. (1), *i.e.*, the antiferro-type nematic interaction that is equivalent to the antiferroelectric polarization. It is consistent with the zero polarization along Z direction at $H = 0$ Oe previously reported[12, 13]. Indeed the calculation of the polarization curve assuming antiferroelectric polarization was consistent with the experiment[17]. The structure of spin dipole, spin nematic operator, and the electric polarization is depicted in Fig. 1(b).

To estimate the spin nematic interaction $J_p^{\rm eff}$, we performed the calculation of magnetic dispersion relation and magnetic susceptibility as displayed in Figs. 2(b), (c) and (d). Main magnetic parameters including exchange constant and single ion anisotropy along z-direction are separately obtained that will be explained later. The dispersion is reproduced by the main parameters plus $J_p^{\rm eff} = -0.198\mu$eV as shown by white solid curve. The calculated susceptibility by using the same parameters in the neutron spectrum is shown in the lower panel of Fig. 2(d) and it reasonably reproduces the experiment. Hence the magnetic anisotropy observed both in the neutron spectrum and bulk magnetic susceptibility is consistently explained by introducing the antiferro-nematic spin interaction.

To determine the main magnetic parameters, inelastic neutron scattering spectra for extended energy transfers were measured as shown in Fig. 3. In addition to the low energy excitations at $0 \lesssim \hbar\omega \lesssim 2$ meV reported in a previous neutron scattering study[11], a new excitation at $\hbar\omega \sim 4$ meV is observed, which corresponds to an electric-field active mode confirmed by electromagnetic wave absorption experiments[20, 21]. The excitation energies obtained by the Gaussian fits to the constant-Q scans are plotted in Figs. 4(a) and (c). Obtained intensities for the excitations are also plotted in Figs. 4(b) and (d). While the lower energy modes at $\hbar\omega \lesssim 2$ meV are explained by a classical spin-wave theory for square-lattice antiferromagnet, the higher energy modes cannot be reproduced. To analyze all the modes we use extended spin-wave theory[22] that is equivalent to the bond operator formulation[18, 23, 24]. We consider the Hamiltonian

$$\mathcal{H} = \sum_i \mathcal{H}_{\rm intra}(i) + \sum_{<i,j>} \mathcal{H}_{\rm inter}(i,j) \tag{3}$$

where $\mathcal{H}_{\rm intra}(i)$ and $\mathcal{H}_{\rm inter}(i,j)$ are Hamiltonians for intrasite and intersite parts defined by

$$\mathcal{H}_{\rm intra}(i) = D(S_i^z)^2 - \sum_{\alpha=x,y,z} g^\alpha \mu_B H^\alpha S_i^\alpha \tag{4}$$

$$\mathcal{H}_{\rm inter}(i,j) = \sum_{\alpha=x,y,z} J^\alpha S_i^\alpha S_j^\alpha + D_{\rm DM}^z(i,j)(S_i^xS_j^y - S_i^yS_j^x) + \mathcal{H}_p \tag{5}$$

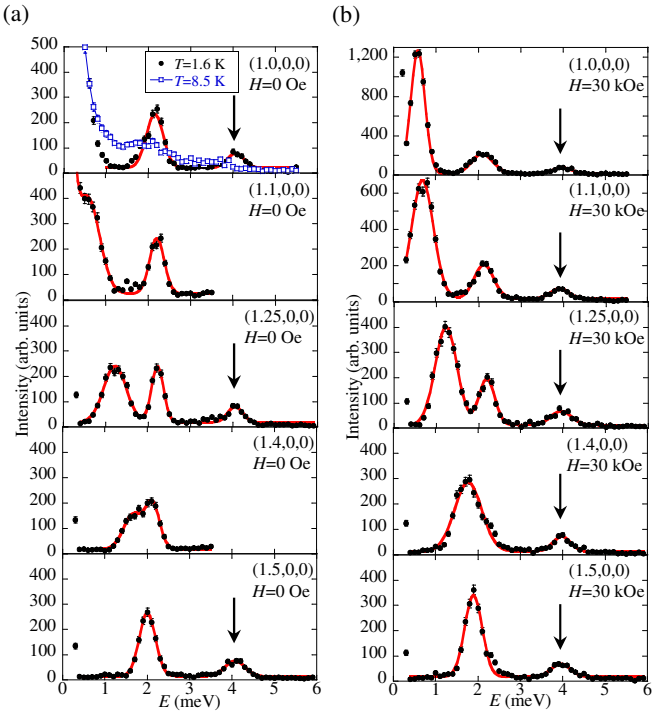

FIG. 3. Typical constant-Q scans at H = 0 Oe and 30 kOe obtained by using TASP spectrometer in PSI. Filled circles are the data at T = 1.6 K and open squares are those at T = 8.5 K. Red solid curves are fits to the data by Gaussian functions.

Here, S_i^α is an $\alpha(= x, y, z)$ component of the $S = 3/2$ spin operator at the i-th site. In the presence of large D, the local energy eigenstates are split into two doublets of $S^z = \pm 1/2$ and $\pm 3/2$. For $D > 0$, $S^z = \pm 1/2$ doublet is stabilized and through intersite interaction an effective $S = 1/2$ spin wave is induced in the low energy range. Further, crystal field like excitation from $S^z = \pm 1/2$ to $\pm 3/2$ exists at higher energy.

As the result of neutron cross section analysis, we obtain the parameters summarized in Table I, which are semi-quantitatively consistent with those obtained from ESR studies[18]. The spin system is approximately identified as $S = 3/2$ square-lattice antiferromagnet with large positive D. Calculated dispersion of the magnetic excitation along $\boldsymbol{Q} = (h,0,0)$ for H=0 Oe and 30 kOe are shown in Figs. 4(a) and (c) by solid curves. The lowest- and second lowest-lying modes are basically connected to the interacting lowest-lying doublets of the $S^z = \pm 1/2$. The former is the transverse fluctuation in the a-b plane, T_1-mode and the latter are those in the c-direction, T_2-mode as depicted in Fig. 4(e). On the other hand, the mode around 4 meV comes from the higher-lying doublets and contains a large magnitude of longitudinal fluctuations of the ordered moment, L-mode [18, 24] and a small magnitude of transverse fluctuations, T_1- and T_2-modes. These L, T_1, and T_2 modes are consistent with those identified in the previous ESR studies[18].

TABLE I. Parameters obtained by extended spin wave calculations.

J^x, J^y (meV)	J^z (meV)	D (meV)	$J_p^{\rm eff}$ (μeV)	$D_{\rm DM}^z$ (μeV)
0.208	0.253	1.034	-0.198	8.61

The existence of spin nematic interaction in multiferroic compound $Ba_2CoGe_2O_7$ was revealed for the first time by a combination of inelastic neutron scattering and bulk magnetization measurements. Several key features in this compound make the physics very interesting; strong SO interaction, the metal-ligand symmetry with no inversion center, and absence of conventional in-plane anisotropy. In the course of this study, we have emphasized that such circumstances result in a characteristic correlation among spin nematic, spin dipole, electric polarization, which is totally described in the spin basis. Using this framework, we succeeded in determining the dielectric energy by measuring precisely the magnetic anisotropy energy.

From magnetic point of view the electric field tunes the direction of magnetic moment and the determined dielectric energy can be a performance index for multiferroicity. Further search for magnets that exhibit small magnetic anisotropy, and therefore small electric field for achieving ferroelectricity, would lead a practical multiferroic device that switches the direction of spin moment by a small electric field.

Prof. A. Zheludev and Dr. S. Gvasaliya are greatly appreciated for facilitating the neutron scattering experiment and for fruitful discussion. This work was supported by KAKENHI (24340077, 20740171, 24740224, and 23540390).

* masuda@issp.u-tokyo.ac.jp

[1] G. A. Smolenskii and I. E. Chupis, Sov. Phys. Usp. **25**, 475 (1982).
[2] M. Fiebig, J. Phys. D: Appl. Phys. **38**, R123 (2005).
[3] W. Eerenstein, N. D. Mathur, and J. F. Scott, Nature **442**, 759 (2006).
[4] T. Kimura, T. Goto, H. Shintani, K. Ishizaka, T. Arima, and Y. Tokura, Nature **426**, 55 (2003).
[5] H. Katsura, N. Nagaosa, and A. V. Balatsky, Phys. Rev. Lett. **95**, 057205 (2005).
[6] M. Mostovoy, Phys. Rev. Lett. **96**, 067601 (2006).
[7] I. A. Sergienko and E. Dagotto, Phys. Rev. B **73**, 094434 (2006).
[8] C. Jia, S. Onoda, N. Nagaosa, and J. H. Han, Phys. Rev. B **76**, 144424 (2007).
[9] T. Arima, J. Phys. Soc. Jpn. **76**, 073702 (2007).
[10] T. Sato, T. Masuda, and K. Uchinokura, Physica B **329–333**, 880 (2003).
[11] A. Zheludev, T. Sato, T. Masuda, K. Uchinokura, G. Shirane, and B. Roessli, Phys. Rev. B **68**, 024428 (2003).

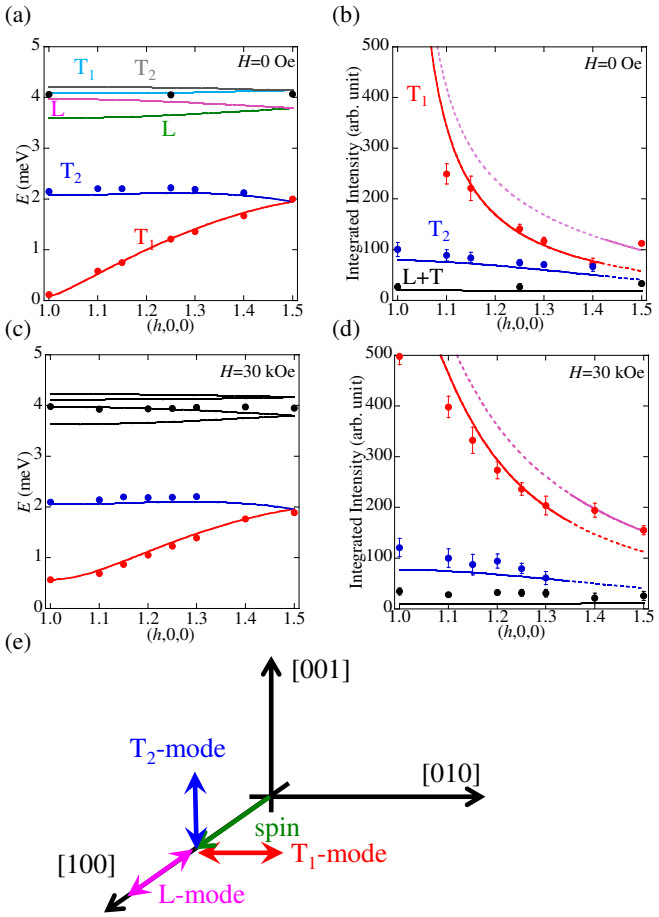

FIG. 4. (a) Magnon dispersion relation for $\mathbf{Q}$=(h,0,0) at H = 0 Oe. (b) Intensity of the inelastic neutron scattering at H = 0 Oe. (c),(d) Magnon dispersion and intensity for H=30 kOe. In each figure the theoretical calculations are indicated by curves and the experimental data are indicated by filled circles. The pink curves in (b) and (d) represent the added intensities of the lowest (red) and the second-lowest (blue) modes for the data of which the energies are close to each other. Similarly the black curves in (b) and (d) are the results after adding all contributions from the four high-energy modes around 4 meV. (e) Schematics of spin fluctuation for each mode at 0 Oe. Transverse fluctuation in the a - b plane is named T_1 mode, those along the c direction is named T_2 mode, and longitudinal fluctuation is named L mode.

[12] H. Murakawa, Y. Onose, S. Miyahara, N. Furukawa, and Y. Tokura, Phys. Rev. Lett. **105**, 137202 (2010).

[13] H. Murakawa, Y. Onose, S. Miyashita, N. Furukawa, and Y. Tokura, Phys. Rev. B **85**, 174106 (2012).

[14] H. T. Yi, Y. J. Choi, and S. W. Cheong, Appl. Phys. Lett. **92**, 212904 (2008).

[15] J. M. Perez-Mato and J. L. Ribeiro, Acta Cryst. A **67**, 264 (2011).

[16] S. Bordács, I. Kézsmárki, D. Szaller, L. Demkó, N. Kida, H. Murakawa, Y. Onose, R. Shimano, T. Rõõm, U. Nagel, et al., Nature Physics **8**, 734 (2012).

[17] J. Romhányi, M. Lajkó, and K. Penc, Phys. Rev. B **84**, 224419 (2011).

[18] K. Penc, J. Romhányi, T. Rõõm, U. Nagel, A. Antal, T. Fehér, A. Jánossy, H. Engelkamp, H. Murakawa, Y. Tokura, et al., Phys. Rev. Lett. **108**, 257203 (2012).

[19] These representations can be also obtained by using the relation between the polarization $\mathbf{P}$, spin moment $\mathbf{S}$, and the position vector of ligands $\mathbf{e}_i$, $\mathbf{P} \propto \Sigma_i (\mathbf{S}\cdot\mathbf{e}_i)^2 \mathbf{e}_i$.

[20] S. Miyahara and N. Furukawa, J. Phys. Soc. Jpn. **80**, 073708 (2011).

[21] I. Kezsmárki, N. Kida, H. Murakawa, S. Bordacs, Y. Onose, and Y. Tokura, Phys. Rev. Lett. **106**, 057403 (2011).

[22] R. Shiina, H. Shiba, P. Thalmeier, A. Takahashi, and O. Sakai, J. Phys. Soc. Jpn. **72**, 1216 (2003).

[23] S. Sachdev and R. N. Bhatt, Phys. Rev. B **41**, 9323 (1990).

[24] J. Romhányi and K. Penc, Phys. Rev. B **86**, 174428 (2012).